1-1-2010

International Geomagnetic Reference Field: the eleventh generation

C. C. Finlay
Institut für Geophysik, cfinlay@erdw.ethz.ch

S. Maus
University of Colorado

C. D. Beggan
British Geological Survey

T. N. Bondar
Pushkov Institute of Terrestrial Magnetism

A. Chambodut
Institut de Physique du Globe de Strasbourg

See next page for additional authors

Authors

C. C. Finlay, S. Maus, C. D. Beggan, T. N. Bondar, A. Chambodut, T. A. Chernova, A. Chulliat, V. P. Golovkov, B. Hamilton, M. Hamoudi, R. Holme, G. Hulot, W. Kuang, B. Langlais, V. Lesur, F. J. Lowes, H. Lühr, S. Macmillan, M. Mandea, S. McLean, C. Manoj, M. Menvielle, I. Michaelis, N. Olsen, J. Rauberg, M. Rother, T. J. Sabaka, A. Tangborn, L. Tøffner-Clausen, E. Thébault, A. W. P. Thomson, I. Wardinski, Z. Wei, and T. I. Zvereva

GJI Geomagnetism, rock magnetism and palaeomagnetism

International Geomagnetic Reference Field: the eleventh generation

International Association of Geomagnetism and Aeronomy, Working Group V-MOD.
Participating members: C. C. Finlay,[1]* S. Maus,[2]* C. D. Beggan,[3] T. N. Bondar,[4]*
A. Chambodut,[5,]* T. A. Chernova,[4] A. Chulliat,[6] V. P. Golovkov,[4] B. Hamilton,[3]
M. Hamoudi,[7] R. Holme,[8] G. Hulot,[6] W. Kuang,[9] B. Langlais,[10] V. Lesur,[7,]*
F. J. Lowes,[11,]* H. Lühr,[7] S. Macmillan,[3,]* M. Mandea,[12] S. McLean,[2,]* C. Manoj,[2]
M. Menvielle,[13] I. Michaelis,[7] N. Olsen,[14,]* J. Rauberg,[7] M. Rother,[7] T. J. Sabaka,[9,]*
A. Tangborn,[15] L. Tøffner-Clausen,[14] E. Thébault,[6,]* A. W. P. Thomson,[3] I. Wardinski,[7]
Z. Wei[15] and T. I. Zvereva[4]

[1]*Earth and Planetary Magnetism Group, Institut für Geophysik, Sonneggstrasse 5, ETH Zürich CH-8092, Switzerland. E-mail: cfinlay@erdw.ethz.ch*
[2]*NOAA/NGDC and CIRES, University of Colorado, USA*
[3]*British Geological Survey, Murchison House, West Mains Road, Edinburgh EH9 3LA, UK*
[4]*Pushkov Institute of Terrestrial Magnetism, Ionosphere and Radio Wave Propagation, IZMIRAN, Troitsk, Moscow Reg. 142190, Russia*
[5]*Institut de Physique du Globe de Strasbourg (UMR 7516-CNRS, Université de Strasbourg/EOST), Strasbourg, France*
[6]*Équipe de G éomagnétisme, Institut de Physique du Globe de Paris, UMR 7154, CNRS/INSU, Univ. Paris Diderot, Paris, France*
[7]*Helmholtz Centre Potsdam, GFZ German Research Centre for Geosciences, Telegrafenberg, 14473 Potsdam, Germany*
[8]*School of Environmental Sciences, University of Liverpool, UK*
[9]*Planetary Geodynamics Laboratory, NASA GSFC, Greenbelt/MD, USA*
[10]*Laboratoire de Planétologie et Géodynamique de Nantes (UMR 6112-CNRS, Université de Nantes), Nantes, France*
[11]*School of Chemistry, University of Newcastle, Newcastle Upon Tyne NE1 7RU, UK*
[12]*Université Paris Diderot, IPG Paris, Géophysique spatiale et planétaire,Bâtiment Lamarck, 5 Rue Thomas Mann, 75013 Paris, France*
[13]*Université Versailles St-Quentin; CNRS/ INSU, LATMOS-IPSL, Paris, France and Département des Sciences de la Terre, Univ. Paris Sud, Orsay, France*
[14]*DTU Space, Juliane Maries Vej 30, 2100 Copenhagen, Denmark*
[15]*Joint Center for Earth Systems Technology, UMBC, USA*

SUMMARY

The eleventh generation of the International Geomagnetic Reference Field (IGRF) was adopted in December 2009 by the International Association of Geomagnetism and Aeronomy Working Group V-MOD. It updates the previous IGRF generation with a definitive main field model for epoch 2005.0, a main field model for epoch 2010.0, and a linear predictive secular variation model for 2010.0–2015.0. In this note the equations defining the IGRF model are provided along with the spherical harmonic coefficients for the eleventh generation. Maps of the magnetic declination, inclination and total intensity for epoch 2010.0 and their predicted rates of change for 2010.0–2015.0 are presented. The recent evolution of the South Atlantic Anomaly and magnetic pole positions are also examined.

Key words: Magnetic field; Satellite magnetics.

1 INTRODUCTION

The International Geomagnetic Reference Field (IGRF) is an established numerical model used to calculate the large scale, internal, part of the Earth's magnetic field at times between 1900.0 A.D. and present, at locations on or above Earth's surface. It is produced and maintained by a team of geomagnetic field modellers under the auspices of the International Association of Geomagnetism and

Aeronomy (IAGA) Working Group V-MOD and is derived from observations collected by satellites, at magnetic observatories, and during magnetic surveys. It is used by scientists (e.g. in studies of space weather or in investigations of local magnetic anomalies) and also by commercial organizations and private individuals who often use the geomagnetic field as a source of orientation information.

The internal part of the geomagnetic field, which is almost entirely core-generated, undergoes slow, but noticeable, changes on timescales of years to decades. Consequently the IGRF must be revised, typically every five years, to remain up to date and as accurate as possible; Table 1 summarizes details of previous generations

*Member of IGRF-11 Task Force.

Table 1. Summary of IGRF generations, their intervals of validity and related references.

Full name	Short name	Valid for	Definitive for	Reference
IGRF 11th generation	IGRF-11	1900.0–2015.0	1945.0–2005.0	This article
IGRF 10th generation	IGRF-10	1900.0–2010.0	1945.0–2000.0	Maus *et al.* (2005a)
IGRF 9th generation	IGRF-9	1900.0–2005.0	1945.0–2000.0	Macmillan *et al.* (2003)
IGRF 8th generation	IGRF-8	1900.0–2005.0	1945.0–1990.0	Mandea & Macmillan (2000)
IGRF 7th generation	IGRF-7	1900.0–2000.0	1945.0–1990.0	Barton (1997)
IGRF 6th generation	IGRF-6	1945.0–1995.0	1945.0–1985.0	Langel (1992)
IGRF 5th generation	IGRF-5	1945.0–1990.0	1945.0–1980.0	Langel *et al.* (1988)
IGRF 4th generation	IGRF-4	1945.0–1990.0	1965.0–1980.0	Barraclough (1987)
IGRF 3rd generation	IGRF-3	1965.0–1985.0	1965.0–1975.0	Peddie (1982)
IGRF 2nd generation	IGRF-2	1955.0–1980.0	—	IAGA (1975)
IGRF 1st generation	IGRF-1	1955.0–1975.0	—	Zmuda (1971)

of the IGRF. Each generation consists of a series of constituent models at 5-yr intervals, each one of which is designated definitive or non-definitive. Once a constituent model is designated definitive it is called a Definitive Geomagnetic Reference Field (DGRF) and it is not revised in subsequent generations of the IGRF. The non-definitive constituent models are referred to as IGRF models. Note that DGRF models have been produced only for epochs from 1945.0 onwards. For further details concerning the history of the IGRF readers should consult Barton (1997), Maus *et al.* (2005a) or Macmillan & Finlay (2010); here attention will focus on the latest (11th generation) revision. Legacy versions of the IGRF are now available from the online archive located at http://www.ngdc.noaa.gov/IAGA/vmod/igrf_old_models.html. These may be useful, for example, to workers who know that a previous generation IGRF has been subtracted from their data and who wish to recover the original data or recorrect it with a more recent reference field.

The 11th generation of the IGRF (hereafter IGRF-11) was agreed in December 2009 by a task force of IAGA Working Group V-MOD. The purpose of this note is to document the release of IGRF-11, to act as a permanent published record of model coefficients and to briefly describe the large-scale features of the present geomagnetic field at Earth's surface as revealed by the updated model.

2 MATHEMATICAL FORMULATION OF THE IGRF MODEL

On and above the Earth's surface, the IGRF model represents the geomagnetic field $\mathbf{B}(r, \theta, \phi, t)$ produced by internal sources in terms of a scalar potential $V(r, \theta, \phi, t)$. We then have $\mathbf{B} = -\nabla V$ where V is a finite series having the numerical Gauss coefficients g_n^m, h_n^m (conventionally given in units of nanotesla, hereafter nT):

$$V(r, \theta, \phi, t) = a \sum_{n=1}^{N} \sum_{m=0}^{n} \left(\frac{a}{r}\right)^{n+1} \left[g_n^m(t) \cos m\phi + h_n^m(t) \sin m\phi\right]$$
$$\times P_n^m(\cos\theta). \tag{1}$$

Here r denotes the radial distance from the centre of the Earth in units of km, $a = 6371.2$ km is the magnetic reference spherical radius which is close to the mean Earth radius, θ denotes geocentric co-latitude (i.e. $90° -$ latitude), and ϕ denotes east longitude. When converting between geocentric and geodetic coordinates, it is recommended to use the World Geodetic System 1984 datum and spheroid (major axis A of 6378.137 km and a reciprocal flattening $1/f$ of 298.257223563). $P_n^m(\cos\theta)$ are the Schmidt semi- (or quasi-) normalized associated Legendre functions of degree n and order m (see, e.g. Winch *et al.* 2005). The maximum spherical har-

monic degree of the expansion N is chosen so that the coefficients of the model are reliably determined given the available coverage and quality of observations. For IGRF-11, N was chosen to be 10 up to and including epoch 1995.0, thereafter it is extended to degree 13 to take advantage of the excellent data provided by the Ørsted and CHAMP satellites.

In the IGRF model, Gauss coefficients g_n^m and h_n^m are provided for the main field (MF) at epochs separated by 5-yr intervals between 1900.0 and 2010.0 A.D. The time-dependence of the Gauss coefficients is then specified using the following linear expression:

$$g_n^m(t) = g_n^m(T_0) + \dot{g}_n^m(T_0)(t - T_0), \tag{2}$$

and similarly for h_n^m. Here t is the time of interest (in units of years) and T_0 is the epoch preceding t which is an exact multiple of 5 yr, such that $T_0 \leq t < (T_0 + 5.0)$. The coefficients $\dot{g}_n^m(T_0)$, given in units of nT yr^{-1}, denote the average first time derivative of $g_n^m(t)$ during the interval T_0 to $T_0 + 5.0$, i.e. the linear secular variation (SV) during this interval. When MF models exist for both T_0 and $T_0 + 5.0$ then $\dot{g}_n^m(T_0)$ is simply calculated using linear interpolation as $[g_n^m(T_0 + 5.0) - g_n^m(T_0)]/5.0$. For the final 5 yr of the model validity (between 2010.0 and 2015.0 for IGRF-11) coefficients of predictive average SV $\dot{g}_n^m(t)$ and $\dot{h}_n^m(t)$ are explicitly provided.

The geocentric components of the geomagnetic field in the northward, eastward and radially inwards directions (X', Y' and Z') are obtained from the model coefficients using eq. (1) and by taking appropriate components of the gradient of V in spherical polar coordinates,

$$X' = \frac{1}{r}\frac{\partial V}{\partial \theta}, \quad Y' = -\frac{1}{r\sin\theta}\frac{\partial V}{\partial \phi}, \quad Z' = \frac{\partial V}{\partial r}. \tag{3}$$

It is often necessary to work in geodetic coordinates and to use the World Geodetic System 1984 datum defined above. Transformations from geocentric to geodetic coordinates and from the geocentric field components (X', Y', Z') into the geodetic field components (X, Y, Z) are described by eqs (1)–(4) of Hulot *et al.* (2007). Often the declination D, inclination I, the horizontal intensity H and the total intensity F are required for applications; these are obtained from X, Y and Z using the relations,

$$H = \sqrt{X^2 + Y^2}, \quad F = \sqrt{X^2 + Y^2 + Z^2},$$
$$D = \arctan(Y/X), \quad I = \arctan(Z/H). \tag{4}$$

3 THE 11TH GENERATION IGRF

In May 2009, the IGRF-11 task force appointed by IAGA Division V-MOD issued a call for candidate models. Candidates for the Definitive Geomagnetic Reference Field (DGRF) for epoch 2005.0,

for a provisional IGRF model for epoch 2010.0, and for a predictive SV model for the interval 2010.0–2015.0 were requested. Candidates were received in early October 2009. Seven candidates were submitted for the DGRF epoch 2005.0 and IGRF epoch 2010.0 MF models. Team A was led by DTU Space, Denmark, along with workers from IPGP, France, and GSFC-NASA, USA; Team B was led by NGDC/NOAA, USA together with colleagues from GFZ, Germany; Team C was from BGS, UK; Team D was from IZMI-RAN, Russia; Team E was led by EOST, France, with assistance from colleagues at LPGN, IPGP and LATMOS, France; Team F was led by IPGP, France, with input from workers in NGDC/NOAA, USA and LPGN, EOST and LATMOS, France; Team G was from GFZ, Germany. The same teams also contributed candidate predictive SV models and there was one additional SV candidate from Team led by GSFC-NASA, USA, in collaboration with UMBC, USA, and University of Liverpool, UK; in all, eight SV candidates were received.

The MF candidate models had a maximum spherical harmonic degree $N = 13$, whereas the task force voted to retain a maximum degree of $N = 8$ for the predictive SV models. The candidate models together with brief descriptions provided by the authors may be obtained from the web page http://www.ngdc.noaa. gov/IAGA/vmod/candidatemodels.html. Papers providing fuller descriptions of the candidate models and detailing the evaluations carried out by the task force (similar to the analysis of the candidates contributing to IGRF-10 carried out by Maus *et al.* 2005b) will appear in a forthcoming special issue of Earth, Planets and Space.

The final IGRF-11 MF models for epochs 2005.0 and 2010.0 as well as the predictive SV model for 2010.0–2015.0 were calculated using weighted means of the candidates. The weights were agreed by a vote of the IGRF-11 task force based on information gleaned from model evaluations, more details of which are documented in Finlay *et al.* (2010).

High-quality, globally distributed, observations of the geomagnetic field are essential to the production of an accurate IGRF revision. The collection of the required comprehensive set of observations involves a significant international collaborative effort. The availability of satellite measurements, from the CHAMP (Reigber *et al.* 2002), Ørsted (Neubert *et al.* 2001) and SAC-C missions, and observatory measurements (see Table A1 in the appendix) was of fundamental importance to IGRF-11.

IGRF-11 remains unchanged from IGRF-10 for epoch 2000.0 and earlier. The model MF coefficients are rounded to 1 nT for epochs between 1900.0 and 1995.0; to 0.1 nT for epochs 2000.0 and 2010.0, and to 0.01 nT for DGRF 2005.0 reflecting the increasing consistency of the candidate models (Finlay *et al.* 2010). The predictive SV coefficients are rounded to the nearest 0.1 nT yr^{-1}. Note that although the formal root mean square (rms) error in DGRF 2005.0 (based on the internal consistency of the contributing candidates) was only 1.0 nT, the true error, due to errors of commission not including unmodelled sources in the Earth's crust and magnetosphere, is probably closer to 5 nT. The error in IGRF-2010 is expected to be slightly larger (approximately 10 nT) because extrapolation of models from submission in October 2009 forward to 2010 was necessary (Lowes 2000). Regarding the predictive SV model, retrospective analysis of previous predictions has shown that errors of up to 20 nT yr^{-1} are likely (Maus *et al.* 2005b; Finlay *et al.* 2010). For further details on the limitations of the IGRF and difficulties in estimating its accuracy readers should consult the IGRF 'health warning' found at http://www.ngdc.noaa.gov/IAGA/vmod/igrfhw.html.

4 IGRF-11 MODEL COEFFICIENTS AND MAPS

In Table 2, the Schmidt semi-normalized spherical harmonic coefficients comprising IGRF-11 are listed. Note that IGRF-11 is a field model that spans the interval from 1900.0 to 2015.0; the entire set of MF coefficients at 5-yr intervals between 1900.0 and 2010.0 and predictive SV coefficients for 2010.0–2015.0 are given here to serve as a complete record of the model. Units are nT for the MF models and nT yr^{-1} for the predictive SV model. The coefficients are also available in various file formats at http://www.ngdc.noaa.gov/IAGA/vmod/igrf.html, along with software to compute the magnetic field components at times and locations of interest. IGRF-11 is also available from the world data centres listed in the Appendix.

Maps of the declination D, inclination I and total intensity F at Earth's surface in 2010 are displayed in Fig. 1. Together these quantities completely define the vector magnetic field. Recall that a purely dipolar field would possess two agonic lines (contours of zero D) running north–south, and a single dip equator (contour of zero I) displaced somewhat from the geographic equator. In contrast, the present geomagnetic field possesses a more complex morphology. It has three agonic lines; one that passes approximately north–south through the Americas, one that is located to the east of Asia and continues down through Indonesia and western Australia, and also one that passes down through central Europe extending as far south as Kenya before looping back northwards via India. Moreover, D is small over a large region spanning mid and low latitudes extending from northeastern Africa east to the Philippine islands. The map of I in the middle panel of Fig. 1 displays a distinctive deflection of the dip equator southwards at South America, an offset in the maximum of I from the geographic south pole towards Australia and also a tongue of high I extending westwards from Southern Africa. The map of F in 2010 in the bottom panel of Fig. 1 shows that the regions with highest field intensity are located in Siberia in the northern hemisphere and in the Southern Ocean and Antarctica southwards of Australia in the southern hemisphere. Perhaps the most striking feature of all is the low field intensity anomaly (compared to a dipole field) currently centred around Southern Brazil and Paraguay. This feature is often referred to as the South Atlantic Anomaly, and it is known to have important consequences regarding the impact of space weather on the near-Earth electromagnetic environment (Gledhill 1976; Heirtzler 2002; Facius & Reitz 2007).

All the features mentioned above are well-known from previous global field models; they have existed for at least several hundred years and have slowly evolved to their present configuration (Jackson *et al.* 2000). The current evolution of main field is illustrated in Fig. 2 which shows the IGRF-11 prediction of the average annual rate of change (SV) in the declination D, inclination I and total intensity F between 2010 and 2015. The predicted changes in D are small in the Pacific hemisphere, and consistent with the continuation of the long-established westward motion of field features in the Atlantic hemisphere. Changes in I are predicted to be largest at low latitudes, with the maximum negative change occurring near northeastern Brazil (close to where the dip equator is presently being deflected southwards) while the maximum positive change is predicted to occur close to Southern India. Considering the predicted changes in F, the largest decreases are predicted to the south of eastern North America as well as to the south west of South America. The later involves a continued deepening and westward motion of the South Atlantic Anomaly. The largest increases in F are predicted to take place in the equatorial part of the mid-Atlantic,

Table 2. 11th Generation International Geomagnetic Reference Field. Schmidt semi-normalized spherical harmonic coefficients are listed. Coefficients for degrees $n = 1, 13$ in units of nanotesla are listed for IGRF and definitive DGRF main field models. Coefficients for degrees $n = 1,8$ in units of $nT\ yr^{-1}$ are listed for the predictive secular variation. Undefined coefficients are marked with '–'; these should be set to 0.0 in numerical calculations as in the electronic coefficient files available online at http://www.ngdc.noaa.gov/IAGA/vmod/igrf.html.

g/h	Degree n	Order m	IGRF 1900.0	IGRF 1905.0	IGRF 1910.0	IGRF 1915.0	IGRF 1920.0	IGRF 1925.0	IGRF 1930.0	IGRF 1935.0	IGRF 1940.0	DGRF 1945.0	DGRF 1950.0	DGRF 1955.0	DGRF 1960.0	DGRF 1965.0	DGRF 1970.0	DGRF 1975.0	DGRF 1980.0	DGRF 1985.0	DGRF 1990.0	DGRF 1995.0	DGRF 2000.0	DGRF 2005.0	IGRF 2010.0	SV 2010-15
g	1	0	−31543	−31464	−31354	−31212	−31060	−30926	−30805	−30715	−30654	−30594	−30554	−30500	−30421	−30334	−30220	−30100	−29992	−29873	−29775	−29692	−29619.4	−29554.63	−29496.5	11.4
g	1	1	−2298	−2298	−2297	−2306	−2317	−2318	−2316	−2306	−2292	−2285	−2250	−2215	−2169	−2119	−2068	−2013	−1956	−1905	−1848	−1784	−1728.2	−1669.05	−1585.9	16.7
h	1	1	5922	5909	5898	5875	5845	5817	5808	5812	5821	5810	5815	5820	5791	5776	5737	5675	5604	5500	5406	5306	5186.1	5077.99	4945.1	−28.8
g	2	0	−677	−728	−769	−802	−839	−893	−951	−1018	−1106	−1244	−1341	−1440	−1555	−1662	−1781	−1902	−1997	−2072	−2131	−2200	−2267.7	−2337.24	−2396.6	−11.3
g	2	1	2905	2928	2948	2956	2959	2969	2980	2984	2981	2990	2998	3003	3002	2997	3000	3010	3027	3044	3059	3070	3068.4	3047.69	3026.0	−3.9
h	2	1	−1061	−1086	−1128	−1191	−1259	−1334	−1424	−1520	−1614	−1702	−1810	−1898	−1967	−2016	−2047	−2067	−2129	−2197	−2279	−2366	−2481.6	−2594.50	−2707.7	−23.0
g	2	2	924	1041	1176	1309	1407	1471	1517	1550	1566	1578	1581	1590	1594	1611	1611	1632	1663	1687	1686	1681	1670.9	1657.76	1668.6	2.7
h	2	2	1121	1065	1000	917	823	728	644	586	528	477	381	291	206	114	25	−68	−200	−306	−373	−413	−458.0	−515.43	−575.4	−12.9
g	3	0	1022	1037	1058	1084	1111	1140	1172	1206	1240	1282	1297	1302	1297	1281	1287	1276	1281	1296	1314	1335	1339.6	1336.30	1339.7	1.3
g	3	1	−1469	−1494	−1524	−1559	−1600	−1645	−1692	−1740	−1790	−1834	−1889	−1944	−1992	−2038	−2091	−2144	−2180	−2208	−2239	−2267	−2288.0	−2305.83	−2326.3	−3.9
h	3	1	−330	−357	−389	−421	−445	−462	−480	−494	−499	−499	−476	−462	−414	−404	−366	−333	−336	−310	−284	−262	−227.6	−198.86	−160.5	8.6
g	3	2	1256	1239	1223	1212	1205	1202	1205	1215	1232	1255	1274	1288	1289	1292	1278	1260	1251	1247	1248	1249	1252.1	1246.39	1231.7	−2.9
h	3	2	3	34	62	84	103	119	133	146	163	186	206	216	224	240	251	262	271	284	293	302	293.4	269.72	251.7	−2.9
g	3	3	572	635	705	778	839	881	907	918	916	913	896	882	878	856	838	830	833	829	802	759	714.5	672.51	634.2	−8.1
h	3	3	523	480	425	360	293	229	166	101	43	−11	−46	−83	−130	−165	−196	−223	−252	−297	−352	−427	−491.1	−524.72	−536.8	−2.1
g	4	0	876	880	884	887	889	891	896	903	914	944	954	958	957	957	952	946	938	936	939	940	932.3	920.55	912.6	−1.4
g	4	1	628	643	660	678	695	711	727	744	762	776	792	796	800	804	800	791	782	780	780	780	786.8	797.96	809.0	2.0
h	4	1	195	203	211	218	220	216	205	188	169	144	136	133	135	148	167	191	212	232	247	262	272.6	282.07	286.4	0.4
g	4	2	660	653	644	631	616	601	584	565	550	544	528	510	504	479	461	438	398	361	325	290	250.0	210.65	166.6	−8.9
h	4	2	−69	−77	−90	−109	−134	−163	−195	−226	−252	−276	−278	−274	−278	−269	−266	−265	−257	−249	−240	−236	−231.9	−225.23	−211.2	3.2
g	4	3	−361	−380	−400	−416	−424	−426	−415	−405	−405	−421	−408	−397	−394	−390	−395	−405	−419	−424	−423	−418	−403.0	−379.86	−357.1	4.4
h	4	3	−210	−201	−189	−173	−153	−130	−109	−90	−72	−55	−37	−23	3	13	26	39	53	69	84	97	119.8	145.15	164.4	3.6
g	4	4	134	146	160	178	199	217	234	249	265	304	303	290	269	252	234	216	199	170	141	122	111.3	100.00	89.7	−2.3
h	4	4	−75	−65	−55	−51	−57	−70	−90	−114	−141	−178	−210	−230	−255	−269	−279	−288	−297	−297	−299	−306	−303.8	−305.36	−309.2	−0.8
g	5	0	−184	−192	−201	−211	−221	−230	−237	−241	−241	−253	−240	−229	−222	−219	−216	−218	−218	−214	−214	−214	−218.8	−227.00	−231.1	−0.5
g	5	1	328	328	327	327	326	326	327	329	334	346	349	360	362	358	359	356	357	355	353	352	351.4	354.41	357.2	0.5
h	5	1	−210	−193	−172	−148	−122	−96	−72	−51	−33	−12	3	15	16	19	26	31	46	47	46	46	43.8	42.72	44.7	0.5
g	5	2	264	259	253	245	236	226	218	211	208	194	211	230	242	254	262	264	261	253	245	235	222.3	208.95	200.3	−1.5
h	5	2	53	56	57	58	58	58	60	64	71	95	103	110	125	128	139	148	150	150	154	165	171.9	180.25	188.9	1.5
g	5	3	5	−1	−9	−16	−23	−28	−32	−33	−33	−20	−23	−26	−31	−31	−42	−59	−74	−93	−109	−118	−130.4	−136.54	−141.2	−0.7
h	5	3	−33	−32	−33	−34	−38	−44	−53	−64	−75	−67	−87	−98	−117	−126	−139	−152	−151	−154	−153	−143	−133.1	−123.45	−118.1	0.9
g	5	4	−86	−93	−102	−111	−119	−125	−131	−136	−141	−142	−147	−152	−156	−157	−160	−159	−162	−164	−165	−166	−168.6	−168.05	−163.1	1.3
h	5	4	−124	−125	−126	−126	−125	−122	−118	−115	−113	−119	−122	−121	−114	−97	−91	−83	−78	−75	−69	−55	−39.3	−19.57	0.1	3.7
g	5	5	−16	−26	−38	−51	−62	−69	−74	−76	−76	−82	−76	−69	−63	−62	−56	−49	−48	−46	−36	−17	−12.9	−13.55	−7.7	1.4
h	5	5	3	11	21	32	43	51	58	64	69	82	80	78	81	81	83	88	92	95	97	107	106.3	103.85	100.9	−0.6
g	6	0	63	62	62	61	61	61	60	59	57	59	54	47	46	45	43	45	48	53	53	68	72.3	73.60	72.8	−0.3
g	6	1	61	60	58	57	55	54	53	53	54	57	57	57	58	61	64	66	66	65	67	67	68.2	69.56	68.6	−0.3
h	6	1	−9	−7	−5	−2	0	3	4	4	4	6	−1	−9	−10	−11	−12	−13	−15	−16	−16	−17	−17.4	−20.33	−20.8	−0.1
g	6	2	−11	−11	−11	−10	−10	−9	−9	−8	−7	6	4	3	1	8	15	28	42	51	59	68	74.2	76.74	76.0	−0.3
h	6	2	83	86	89	93	96	99	102	104	105	100	99	96	99	100	100	99	93	88	82	72	63.7	54.75	44.2	−2.1
g	6	3	−217	−221	−224	−228	−233	−238	−242	−246	−249	−246	−247	−247	−237	−228	−212	−198	−192	−185	−178	−170	−160.9	−151.34	−141.4	1.9
h	6	3	2	4	5	8	11	14	19	25	33	16	33	48	60	68	72	75	71	69	69	67	65.1	63.63	61.5	−0.4
g	6	4	−58	−57	−54	−51	−46	−40	−32	−25	−18	−25	−16	−8	−1	4	2	1	4	4	3	−1	−5.9	−14.58	−22.9	−1.6
h	6	4	−35	−32	−29	−26	−22	−18	−15	−15	−18	−9	−12	−16	−20	−32	−37	−41	−43	−48	−52	−58	−61.2	−63.53	−66.3	−0.5
g	6	5	59	57	54	49	44	39	32	25	18	21	12	7	2	1	3	6	14	16	18	19	16.9	14.58	13.1	−0.2
h	6	5	36	32	28	23	18	13	8	4	0	−16	−12	−12	−11	−8	−6	−4	−2	−1	1	1	0.7	0.24	3.1	0.8

Table 2. (*Continued.*)

Degree n	Order m	g/h	IGRF 1900.0	IGRF 1905.0	IGRF 1910.0	IGRF 1915.0	IGRF 1920.0	IGRF 1925.0	IGRF 1930.0	IGRF 1935.0	IGRF 1940.0	DGRF 1945.0	DGRF 1950.0	DGRF 1955.0	DGRF 1960.0	DGRF 1965.0	DGRF 1970.0	DGRF 1975.0	DGRF 1980.0	DGRF 1985.0	DGRF 1990.0	DGRF 1995.0	DGRF 2000.0	DGRF 2005.0	IGRF 2010.0	SV 2010-15
6	6	g	-90	-92	-95	-98	-101	-103	-104	-106	-107	-104	-105	-107	-113	-111	-112	-111	-108	-102	-96	-93	-90.4	-86.36	-77.9	1.8
6	6	h	-69	-67	-65	-62	-57	-52	-46	-40	-33	-39	-30	-24	-17	-7	1	11	17	21	24	36	43.8	50.94	54.9	0.5
7	0	g	70	70	71	72	73	73	74	74	74	70	65	65	67	75	72	71	72	74	77	77	79.0	79.88	80.4	0.2
7	1	g	-55	-54	-54	-54	-54	-54	-54	-53	-53	-40	-55	-56	-56	-57	-57	-56	-59	-62	-64	-72	-74.0	-74.46	-75.0	-0.1
7	1	h	-45	-46	-47	-48	-49	-50	-51	-52	-52	-45	-35	-50	-55	-61	-70	-77	-82	-83	-80	-69	-64.6	-61.14	-57.8	0.6
7	2	g	0	0	1	2	2	3	4	4	4	0	2	2	5	4	1	1	2	3	2	1	0.0	-1.65	-4.7	-0.6
7	2	h	-13	-14	-14	-14	-14	-14	-15	-17	-18	-18	-17	-24	-28	-27	-27	-26	-27	-27	-26	-25	-24.2	-22.57	-21.2	0.3
7	3	g	34	33	32	31	29	27	25	23	20	0	1	10	15	13	14	16	21	24	26	28	33.3	38.73	45.3	1.4
7	3	h	-10	-11	-12	-12	-13	-14	-14	-14	-14	2	0	-4	-6	-2	-4	-5	-5	-2	0	4	6.2	6.82	6.6	-0.2
7	4	g	-41	-41	-40	-38	-37	-35	-34	-33	-31	-29	-40	-32	-32	-26	-22	-14	-12	-6	-1	5	9.1	12.30	14.0	0.3
7	4	h	-1	0	1	2	4	5	6	7	7	6	10	8	7	6	8	10	16	20	21	24	24.0	25.35	24.9	-0.1
7	5	g	-21	-20	-19	-18	-16	-14	-12	-11	-9	-10	-7	-11	-7	-6	-2	0	1	4	5	4	6.9	9.37	10.4	0.1
7	5	h	28	28	28	28	28	29	29	29	29	28	36	28	23	26	23	22	18	17	17	17	14.8	10.93	7.0	-0.8
7	6	g	18	18	18	19	19	19	18	18	17	15	5	9	17	13	13	12	11	10	9	8	7.3	5.42	1.6	-0.8
7	6	h	-12	-12	-13	-15	-16	-17	-18	-19	-20	-17	-18	-20	-18	-23	-23	-23	-23	-23	-23	-24	-25.4	-26.32	-27.7	-0.3
7	7	g	6	6	6	6	6	6	6	6	5	29	19	18	8	1	-2	-5	-2	0	0	-2	-1.2	1.94	4.9	0.4
7	7	h	-22	-22	-22	-22	-22	-21	-20	-19	-19	-22	-16	-18	-17	-12	-11	-12	-10	-7	-4	-6	-5.8	-4.64	-3.4	0.2
8	0	g	11	11	11	11	11	11	11	11	11	13	11	11	15	13	14	14	18	21	23	25	24.4	24.80	24.3	-0.1
8	1	g	8	8	8	8	7	7	7	7	7	7	15	9	6	5	6	6	6	6	5	6	6.6	7.62	8.2	0.1
8	1	h	8	8	8	8	8	8	8	8	8	12	5	10	11	7	7	6	7	8	10	11	11.9	11.20	10.9	0.0
8	2	g	-4	-4	-4	-4	-3	-3	-3	-3	-3	-8	-4	-6	-4	-4	-2	-1	0	0	-1	-6	-9.2	-11.73	-14.5	-0.5
8	2	h	-14	-15	-15	-15	-15	-15	-15	-15	-15	-21	-22	-15	-14	-12	-15	-16	-18	-19	-19	-21	-21.5	-20.88	-20.0	0.2
8	3	g	-9	-9	-9	-9	-9	-9	-10	-11	-12	-5	-1	-14	-11	-14	-13	-12	-11	-11	-10	-9	-7.9	-6.88	-5.7	0.3
8	3	h	7	7	6	6	6	6	5	5	5	-12	0	5	7	9	6	4	4	5	6	8	8.5	9.83	11.9	0.5
8	4	g	1	1	1	2	2	2	2	1	1	9	11	6	2	0	-3	-8	-7	-9	-12	-14	-16.6	-18.11	-19.3	-0.3
8	4	h	-13	-13	-13	-13	-14	-14	-14	-15	-15	-7	-21	-23	-18	-16	-17	-19	-22	-23	-22	-23	-21.5	-19.71	-17.4	0.4
8	5	g	2	2	2	3	4	4	5	6	6	7	15	10	10	8	5	4	4	4	3	4	9.1	10.17	11.6	0.3
8	5	h	5	5	5	5	5	5	5	5	5	2	-8	3	4	4	6	6	9	11	12	15	15.5	16.22	16.7	0.1
8	6	g	-9	-8	-8	-8	-7	-7	-6	-6	-6	-10	-13	-7	-5	-1	0	0	3	4	4	6	7.0	9.36	10.9	0.2
8	6	h	16	16	16	16	17	17	18	18	19	18	17	23	23	24	21	18	16	14	12	11	8.9	7.61	7.1	-0.1
8	7	g	5	5	5	6	6	7	8	8	8	7	5	6	10	11	11	10	6	4	2	2	-7.9	-11.25	-14.1	-0.5
8	7	h	-5	-5	-5	-5	-5	-5	-5	-6	-6	-5	-1	-4	-3	-3	-6	-5	-1	1	2	5	-14.9	-12.76	-10.8	0.4
8	8	g	8	8	8	8	8	8	8	8	8	7	9	5	8	8	3	1	-1	-4	-6	-7	-7.0	-4.87	-3.7	0.2
8	8	h	-18	-18	-18	-18	-19	-19	-19	-19	-19	-13	-20	-13	-20	-17	-16	-17	-15	-11	-10	-4	-2.1	-0.06	1.7	0.4
9	0	g	8	8	8	8	8	8	8	8	8	5	3	4	4	4	4	8	5	5	4	4	5.0	5.58	5.4	–
9	1	g	10	10	10	10	10	10	10	10	10	-21	-7	9	6	5	10	10	10	10	9	9	9.4	9.76	9.4	–
9	1	h	-20	-20	-20	-20	-20	-20	-20	-20	-21	-27	-24	-11	-18	-22	-21	-21	-21	-20	-20	-20	-19.7	-20.11	-20.5	–
9	2	g	1	1	1	1	1	1	1	1	1	1	4	-4	0	2	2	2	1	1	1	3	3.0	3.58	3.4	–
9	2	h	14	14	14	14	14	14	14	14	15	17	19	12	12	15	16	16	16	15	15	15	13.4	12.69	11.6	–
9	3	g	-11	-11	-11	-11	-11	-11	-11	-11	-12	-11	-25	-5	-9	-13	-12	-12	-12	-12	-10	-10	-8.4	-6.94	-5.3	–
9	3	h	5	5	5	5	5	5	5	5	5	29	12	7	2	7	9	9	9	11	12	12	12.5	12.67	12.8	–
9	4	g	12	12	12	12	12	12	12	12	11	3	10	2	1	10	9	10	9	9	9	8	6.3	5.01	3.1	–
9	4	h	-3	-3	-3	-3	-3	-3	-3	-3	-3	-9	2	6	0	-4	-5	-4	-5	-6	-6	-6	-6.2	-6.72	-7.2	–
9	5	g	1	1	1	1	1	1	1	1	1	16	5	4	4	-1	-3	-1	-3	-3	-4	-4	-8.9	-10.76	-12.4	–
9	5	h	-2	-2	-2	-2	-2	-2	-2	-2	-3	4	2	-2	-3	-5	-6	-5	-6	-6	-7	-8	-8.4	-8.16	-7.4	–
9	6	g	-2	-2	-2	-2	-2	-2	-2	-2	-2	-3	-5	1	-1	-1	-1	-1	-1	-1	-2	-1	-1.5	-1.25	-0.8	–
9	6	h	8	8	8	8	9	9	9	9	9	9	8	10	9	10	10	10	9	9	9	8	8.4	8.10	8.0	–

Table 2. (*Continued.*)

g/h	n	m	IGRF 1900.0	IGRF 1905.0	IGRF 1910.0	IGRF 1915.0	IGRF 1920.0	IGRF 1925.0	IGRF 1930.0	IGRF 1935.0	IGRF 1940.0	DGRF 1945.0	DGRF 1950.0	DGRF 1955.0	DGRF 1960.0	DGRF 1965.0	DGRF 1970.0	DGRF 1975.0	DGRF 1980.0	DGRF 1985.0	DGRF 1990.0	DGRF 1995.0	DGRF 2000.0	DGRF 2005.0	IGRF 2010.0	SV 2010-15
g	9	7	2	2	2	2	2	2	3	3	3	-4	-2	2	-2	5	3	4	7	7	7	10	9.3	8.76	8.4	–
h	9	7	10	10	10	10	10	10	10	11	11	6	8	7	8	10	11	11	10	9	8	5	3.8	2.92	2.2	–
g	9	8	-1	0	0	0	0	0	0	0	1	-3	3	2	3	0	1	1	2	1	1	-2	-4.3	-6.66	-8.4	–
h	9	8	-2	-2	-2	-1	-2	-2	-2	-2	-2	1	-11	-6	0	-4	-2	-3	-6	-7	-7	-8	-8.2	-7.73	-6.1	–
g	9	9	-1	-1	-1	-1	-1	-1	-2	-2	-2	-4	8	5	-1	-2	-1	-2	-5	-5	-6	-8	-8.2	-9.22	-10.1	–
h	9	9	2	2	2	2	2	2	2	2	2	8	-7	5	5	1	1	1	2	2	2	3	4.8	6.01	7.0	–
g	10	0	-3	-3	-3	-3	-3	-3	-3	-3	-3	-3	-8	-3	1	-2	-3	-3	-4	-4	-3	-3	-2.6	-2.17	-2.0	–
g	10	1	-4	-4	-4	-4	-4	-4	-4	-4	-4	11	4	-5	-3	-3	-3	-3	-4	-4	-4	-6	-6.0	-6.12	-6.3	–
h	10	1	2	2	2	2	2	2	2	2	2	5	13	-4	4	2	2	1	2	1	2	1	1.7	2.19	2.8	–
g	10	2	2	2	2	2	2	2	2	2	2	1	-1	-1	4	2	2	2	2	3	2	2	1.7	1.42	0.9	–
h	10	2	1	1	1	1	1	1	1	1	2	-1	-2	0	0	1	1	1	0	0	1	0	0.0	0.10	-0.1	–
g	10	3	-5	-5	-5	-5	-5	-5	-5	-5	-5	2	13	2	0	-5	-5	-5	-5	-5	-5	-4	-3.1	-2.35	-1.1	–
h	10	3	2	2	2	2	2	2	2	2	2	-20	-10	-8	0	2	3	3	3	3	3	4	4.0	4.46	4.7	–
g	10	4	-2	-2	-2	-2	-2	-2	-2	-2	-2	-5	-4	-3	-1	-2	-1	-2	-2	-2	-2	-1	-0.5	-0.15	-0.2	–
h	10	4	6	6	6	6	6	6	6	6	6	-1	2	-2	2	6	4	4	6	6	6	5	4.9	4.76	4.4	–
g	10	5	6	6	6	6	6	6	6	6	6	-1	4	7	4	4	6	4	5	5	4	4	3.7	3.06	2.5	–
h	10	5	-4	-4	-4	-4	-4	-4	-4	-4	-4	-6	-3	-4	-5	-4	-4	-4	-4	-4	-4	-5	-5.9	-6.58	-7.2	–
g	10	6	4	4	4	4	4	4	4	4	4	8	12	4	6	4	4	4	3	3	3	2	1.0	0.29	-0.3	–
h	10	6	0	0	0	0	0	0	0	0	0	6	6	1	1	0	0	-1	0	0	0	-1	-1.2	-1.01	-1.0	–
g	10	7	0	0	0	0	0	0	0	0	0	-1	3	-2	1	0	1	1	1	1	1	2	2.0	2.06	2.2	–
h	10	7	-2	-2	-2	-2	-2	-2	-2	-1	-1	-4	-3	-3	-1	-2	0	-1	-1	-1	-2	-2	-2.9	-3.47	-4.0	–
g	10	8	2	2	2	1	1	1	1	2	2	-3	2	6	6	2	2	0	2	2	3	5	4.2	3.77	3.1	–
h	10	8	4	4	4	4	4	4	4	4	4	-2	6	7	3	3	3	3	4	4	3	1	0.2	-0.86	-2.0	–
g	10	9	2	2	2	2	3	3	3	3	3	5	10	-2	2	2	3	3	3	3	3	-2	0.3	-0.21	-1.0	–
h	10	9	0	0	0	0	0	0	0	0	0	0	11	-1	0	0	1	1	0	0	-1	0	-2.2	-2.31	-2.0	–
g	10	10	0	0	0	0	0	0	0	0	0	-2	3	0	0	0	-1	-1	0	0	0	0	-1.1	-2.09	-2.8	–
h	10	10	-6	-6	-6	-6	-6	-6	-6	-6	-6	-2	8	-3	-7	-6	-4	-5	-6	-6	-6	-7	-7.4	-7.93	-8.3	–
g	11	0	–	–	–	–	–	–	–	–	–	–	–	–	–	–	–	–	–	–	–	–	2.7	2.95	3.0	–
g	11	1	–	–	–	–	–	–	–	–	–	–	–	–	–	–	–	–	–	–	–	–	-1.7	-1.60	-1.5	–
h	11	1	–	–	–	–	–	–	–	–	–	–	–	–	–	–	–	–	–	–	–	–	0.1	0.26	0.1	–
g	11	2	–	–	–	–	–	–	–	–	–	–	–	–	–	–	–	–	–	–	–	–	-1.9	-1.88	-2.1	–
h	11	2	–	–	–	–	–	–	–	–	–	–	–	–	–	–	–	–	–	–	–	–	1.3	1.44	1.7	–
g	11	3	–	–	–	–	–	–	–	–	–	–	–	–	–	–	–	–	–	–	–	–	1.5	1.44	1.6	–
h	11	3	–	–	–	–	–	–	–	–	–	–	–	–	–	–	–	–	–	–	–	–	-0.9	-0.77	-0.6	–
g	11	4	–	–	–	–	–	–	–	–	–	–	–	–	–	–	–	–	–	–	–	–	-0.1	-0.31	-0.5	–
h	11	4	–	–	–	–	–	–	–	–	–	–	–	–	–	–	–	–	–	–	–	–	-2.6	-2.27	-1.8	–
g	11	5	–	–	–	–	–	–	–	–	–	–	–	–	–	–	–	–	–	–	–	–	0.1	0.29	0.5	–
h	11	5	–	–	–	–	–	–	–	–	–	–	–	–	–	–	–	–	–	–	–	–	0.9	0.90	0.9	–
g	11	6	–	–	–	–	–	–	–	–	–	–	–	–	–	–	–	–	–	–	–	–	-0.7	-0.79	-0.8	–
h	11	6	–	–	–	–	–	–	–	–	–	–	–	–	–	–	–	–	–	–	–	–	-0.7	-0.58	-0.4	–
g	11	7	–	–	–	–	–	–	–	–	–	–	–	–	–	–	–	–	–	–	–	–	-2.8	-2.69	-2.5	–
h	11	7	–	–	–	–	–	–	–	–	–	–	–	–	–	–	–	–	–	–	–	–	0.7	0.53	0.4	–
g	11	8	–	–	–	–	–	–	–	–	–	–	–	–	–	–	–	–	–	–	–	–	1.7	1.80	1.8	–
h	11	8	–	–	–	–	–	–	–	–	–	–	–	–	–	–	–	–	–	–	–	–	-0.9	-1.08	-1.3	–
g	11	9	–	–	–	–	–	–	–	–	–	–	–	–	–	–	–	–	–	–	–	–	0.1	0.16	0.2	–
h	11	9	–	–	–	–	–	–	–	–	–	–	–	–	–	–	–	–	–	–	–	–	-1.2	-1.58	-2.1	–
g	11	10	–	–	–	–	–	–	–	–	–	–	–	–	–	–	–	–	–	–	–	–	1.2	0.96	0.8	–

Table 2. (*Continued.*)

g/h	Degree n	Order m	IGRF 1900.0	IGRF 1905.0	IGRF 1910.0	IGRF 1915.0	IGRF 1920.0	IGRF 1925.0	IGRF 1930.0	IGRF 1935.0	IGRF 1940.0	DGRF 1945.0	DGRF 1950.0	DGRF 1955.0	DGRF 1960.0	DGRF 1965.0	DGRF 1970.0	DGRF 1975.0	DGRF 1980.0	DGRF 1985.0	DGRF 1990.0	DGRF 1995.0	DGRF 2000.0	DGRF 2005.0	IGRF 2010.0	SV 2010-15
h	11	10	–	–	–	–	–	–	–	–	–	–	–	–	–	–	–	–	–	–	–	–	–1.9	–1.90	–1.9	–
g	11	11	–	–	–	–	–	–	–	–	–	–	–	–	–	–	–	–	–	–	–	–	4.0	3.99	3.8	–
h	11	11	–	–	–	–	–	–	–	–	–	–	–	–	–	–	–	–	–	–	–	–	–0.9	–1.39	–1.8	–
g	12	0	–	–	–	–	–	–	–	–	–	–	–	–	–	–	–	–	–	–	–	–	–2.2	–2.15	–2.1	–
g	12	1	–	–	–	–	–	–	–	–	–	–	–	–	–	–	–	–	–	–	–	–	–0.3	–0.29	–0.2	–
h	12	1	–	–	–	–	–	–	–	–	–	–	–	–	–	–	–	–	–	–	–	–	–0.4	–0.55	–0.8	–
g	12	2	–	–	–	–	–	–	–	–	–	–	–	–	–	–	–	–	–	–	–	–	0.2	0.21	0.3	–
h	12	2	–	–	–	–	–	–	–	–	–	–	–	–	–	–	–	–	–	–	–	–	0.3	0.23	0.3	–
g	12	3	–	–	–	–	–	–	–	–	–	–	–	–	–	–	–	–	–	–	–	–	0.9	0.89	1.0	–
h	12	3	–	–	–	–	–	–	–	–	–	–	–	–	–	–	–	–	–	–	–	–	2.5	2.38	2.2	–
g	12	4	–	–	–	–	–	–	–	–	–	–	–	–	–	–	–	–	–	–	–	–	–0.2	–0.38	–0.7	–
h	12	4	–	–	–	–	–	–	–	–	–	–	–	–	–	–	–	–	–	–	–	–	–2.6	–2.63	–2.5	–
g	12	5	–	–	–	–	–	–	–	–	–	–	–	–	–	–	–	–	–	–	–	–	0.9	0.96	0.9	–
h	12	5	–	–	–	–	–	–	–	–	–	–	–	–	–	–	–	–	–	–	–	–	0.7	0.61	0.5	–
g	12	6	–	–	–	–	–	–	–	–	–	–	–	–	–	–	–	–	–	–	–	–	–0.5	–0.30	–0.1	–
h	12	6	–	–	–	–	–	–	–	–	–	–	–	–	–	–	–	–	–	–	–	–	0.3	0.40	0.6	–
g	12	7	–	–	–	–	–	–	–	–	–	–	–	–	–	–	–	–	–	–	–	–	0.3	0.46	0.5	–
h	12	7	–	–	–	–	–	–	–	–	–	–	–	–	–	–	–	–	–	–	–	–	0.0	0.01	0.0	–
g	12	8	–	–	–	–	–	–	–	–	–	–	–	–	–	–	–	–	–	–	–	–	–0.3	–0.35	–0.4	–
h	12	8	–	–	–	–	–	–	–	–	–	–	–	–	–	–	–	–	–	–	–	–	0.0	0.02	0.1	–
g	12	9	–	–	–	–	–	–	–	–	–	–	–	–	–	–	–	–	–	–	–	–	–0.4	–0.36	–0.4	–
h	12	9	–	–	–	–	–	–	–	–	–	–	–	–	–	–	–	–	–	–	–	–	0.3	0.28	0.3	–
g	12	10	–	–	–	–	–	–	–	–	–	–	–	–	–	–	–	–	–	–	–	–	–0.1	0.08	0.2	–
h	12	10	–	–	–	–	–	–	–	–	–	–	–	–	–	–	–	–	–	–	–	–	–0.9	–0.87	–0.9	–
g	12	11	–	–	–	–	–	–	–	–	–	–	–	–	–	–	–	–	–	–	–	–	–0.2	–0.49	–0.8	–
h	12	11	–	–	–	–	–	–	–	–	–	–	–	–	–	–	–	–	–	–	–	–	–0.4	–0.34	–0.2	–
g	12	12	–	–	–	–	–	–	–	–	–	–	–	–	–	–	–	–	–	–	–	–	–0.4	–0.08	0.0	–
h	12	12	–	–	–	–	–	–	–	–	–	–	–	–	–	–	–	–	–	–	–	–	0.8	0.88	0.8	–
g	13	0	–	–	–	–	–	–	–	–	–	–	–	–	–	–	–	–	–	–	–	–	–0.2	–0.16	–0.2	–
g	13	1	–	–	–	–	–	–	–	–	–	–	–	–	–	–	–	–	–	–	–	–	–0.9	–0.88	–0.9	–
h	13	1	–	–	–	–	–	–	–	–	–	–	–	–	–	–	–	–	–	–	–	–	–0.9	–0.76	–0.8	–
g	13	2	–	–	–	–	–	–	–	–	–	–	–	–	–	–	–	–	–	–	–	–	0.3	0.30	0.3	–
h	13	2	–	–	–	–	–	–	–	–	–	–	–	–	–	–	–	–	–	–	–	–	0.2	0.33	0.3	–
g	13	3	–	–	–	–	–	–	–	–	–	–	–	–	–	–	–	–	–	–	–	–	0.1	0.28	0.4	–
h	13	3	–	–	–	–	–	–	–	–	–	–	–	–	–	–	–	–	–	–	–	–	1.8	1.72	1.7	–
g	13	4	–	–	–	–	–	–	–	–	–	–	–	–	–	–	–	–	–	–	–	–	–0.4	–0.43	–0.4	–
h	13	4	–	–	–	–	–	–	–	–	–	–	–	–	–	–	–	–	–	–	–	–	–0.4	–0.54	–0.6	–
g	13	5	–	–	–	–	–	–	–	–	–	–	–	–	–	–	–	–	–	–	–	–	1.3	1.18	1.1	–
h	13	5	–	–	–	–	–	–	–	–	–	–	–	–	–	–	–	–	–	–	–	–	–1.0	–1.07	–1.2	–
g	13	6	–	–	–	–	–	–	–	–	–	–	–	–	–	–	–	–	–	–	–	–	–0.4	–0.37	–0.3	–
h	13	6	–	–	–	–	–	–	–	–	–	–	–	–	–	–	–	–	–	–	–	–	–0.1	–0.04	–0.1	–
g	13	7	–	–	–	–	–	–	–	–	–	–	–	–	–	–	–	–	–	–	–	–	0.7	0.75	0.8	–
h	13	7	–	–	–	–	–	–	–	–	–	–	–	–	–	–	–	–	–	–	–	–	0.7	0.63	0.5	–
g	13	8	–	–	–	–	–	–	–	–	–	–	–	–	–	–	–	–	–	–	–	–	–0.4	–0.26	–0.2	–
h	13	8	–	–	–	–	–	–	–	–	–	–	–	–	–	–	–	–	–	–	–	–	0.3	0.21	0.1	–
g	13	9	–	–	–	–	–	–	–	–	–	–	–	–	–	–	–	–	–	–	–	–	0.3	0.35	0.4	–
h	13	9	–	–	–	–	–	–	–	–	–	–	–	–	–	–	–	–	–	–	–	–	0.6	0.53	0.5	–

Table 2. (*Continued.*)

g/h	Degree n	Order m	IGRF 1900.0	IGRF 1905.0	IGRF 1910.0	IGRF 1915.0	IGRF 1920.0	IGRF 1925.0	IGRF 1930.0	IGRF 1935.0	IGRF 1940.0	DGRF 1945.0	DGRF 1950.0	DGRF 1955.0	DGRF 1960.0	DGRF 1965.0	DGRF 1970.0	DGRF 1975.0	DGRF 1980.0	DGRF 1985.0	DGRF 1990.0	DGRF 1995.0	DGRF 2000.0	DGRF 2005.0	IGRF 2010.0	SV 2010-15
g	13	10	–	–	–	–	–	–	–	–	–	–	–	–	–	–	–	–	–	–	–	–	−0.1	−0.05	0.0	–
h	13	10	–	–	–	–	–	–	–	–	–	–	–	–	–	–	–	–	–	–	–	–	0.3	0.38	0.4	–
g	13	11	–	–	–	–	–	–	–	–	–	–	–	–	–	–	–	–	–	–	–	–	0.4	0.41	0.4	–
h	13	11	–	–	–	–	–	–	–	–	–	–	–	–	–	–	–	–	–	–	–	–	−0.2	−0.22	−0.2	–
g	13	12	–	–	–	–	–	–	–	–	–	–	–	–	–	–	–	–	–	–	–	–	0.0	−0.10	−0.3	–
h	13	12	–	–	–	–	–	–	–	–	–	–	–	–	–	–	–	–	–	–	–	–	−0.5	−0.57	−0.5	–
g	13	13	–	–	–	–	–	–	–	–	–	–	–	–	–	–	–	–	–	–	–	–	0.1	−0.18	−0.3	–
h	13	13	–	–	–	–	–	–	–	–	–	–	–	–	–	–	–	–	–	–	–	–	−0.9	−0.82	−0.8	–

in the southern Indian ocean (south-east of Africa), and in the region encompassing Iran, Kazakhstan, Afghanistan, Pakistan and India. Understanding of the future evolution of these field features requires detailed knowledge of the magnetohydrodynamic processes taking place in the liquid iron outer core. Such processes are only partly understood at present, but are the focus of much active research (see, for example, Olson 2007).

Further details concerning the evolution of the South Atlantic Anomaly since 1900 as captured by IGRF-11 are presented in Fig. 3 (see also Macmillan *et al.* 2009). The left plot shows how the lowest field intensity *F* within the South Atlantic Anomaly has systematically decreased since 1900. The decrease has been almost linear since 1940 (when the weakest intensity was 24 954 nT) until the present (the weakest intensity in 2010 was 22 590 nT) with an average decrease of 34 nT yr^{-1}. There is no sign that the decrease of field intensity in the South Atlantic Anomaly is abating, with a further decrease to 22 430 nT predicted by 2015. The right hand plot documents the motion of the location of this point of lowest field intensity every 5 yr from 1900.0 to 2015.0, where the final point is a prediction. The position of lowest intensity has moved both southward and westward, but almost exclusively westwards since 1955. This analysis describes only the position with lowest intensity; the spatial extent of the south Atlantic anomaly has also increased during the past century, for example as measured by the area within the 28 000 nT contour of *F*. Note however, that the exact position of the lowest intensity point is known only rather crudely, particularly before 1960 when there was larger uncertainty in the field models.

In Fig. 4, we present the positions of the geomagnetic pole (as determined only from the $n = 1$ dipole field coefficients) and the magnetic dip pole (where inclination *I* is vertical, as determined from the entire field model to degree $n = N$) calculated from IGRF-11 and plotted as a function of time since 1900. Pole positions are also tabulated in Table 3. It is noteworthy that the North magnetic dip pole is currently moving at a high speed of over 50 km yr^{-1}, as recently investigated by Newitt *et al.* (2009).

Because of the significant changes currently taking place in the internal geomagnetic field, including the development of the South Atlantic Anomaly and the motions of the geomagnetic poles described above, continued careful monitoring is essential. At the time of writing, the CHAMP and Ørsted satellites that were crucial sources of observations for IGRF-11 are approaching the end of their lifetimes, but fortunately one of the aims of the upcoming ESA Swarm mission (Friis-Christensen *et al.* 2006) is to provide the high-quality satellite data that will be of great importance to the next IGRF revision.

The 11th generation IGRF was computed from candidate models produced and evaluated by participating members of IAGA Working Group V-MOD who are listed as co-authors of this paper. Their institutes and the many organizations involved in operating the magnetic satellites CHAMP, Ørsted and SAC-C, observatories (see the appendix for a list), magnetic survey programmes, and the World Data Centres are thanked for their continued support of the IGRF project.

5 IGRF-11 ONLINE DATA PRODUCTS

Further general information about the IGRF:
http://www.ngdc.noaa.gov/IAGA/vmod/igrf.html.

The coefficients of IGRF-11 in various file formats:
http://www.ngdc.noaa.gov/IAGA/vmod/igrf11coeffs.txt

Declination *D* in degrees in 2010

Inclination *I* in degrees in 2010

Total Intensity *F* in nT in 2010
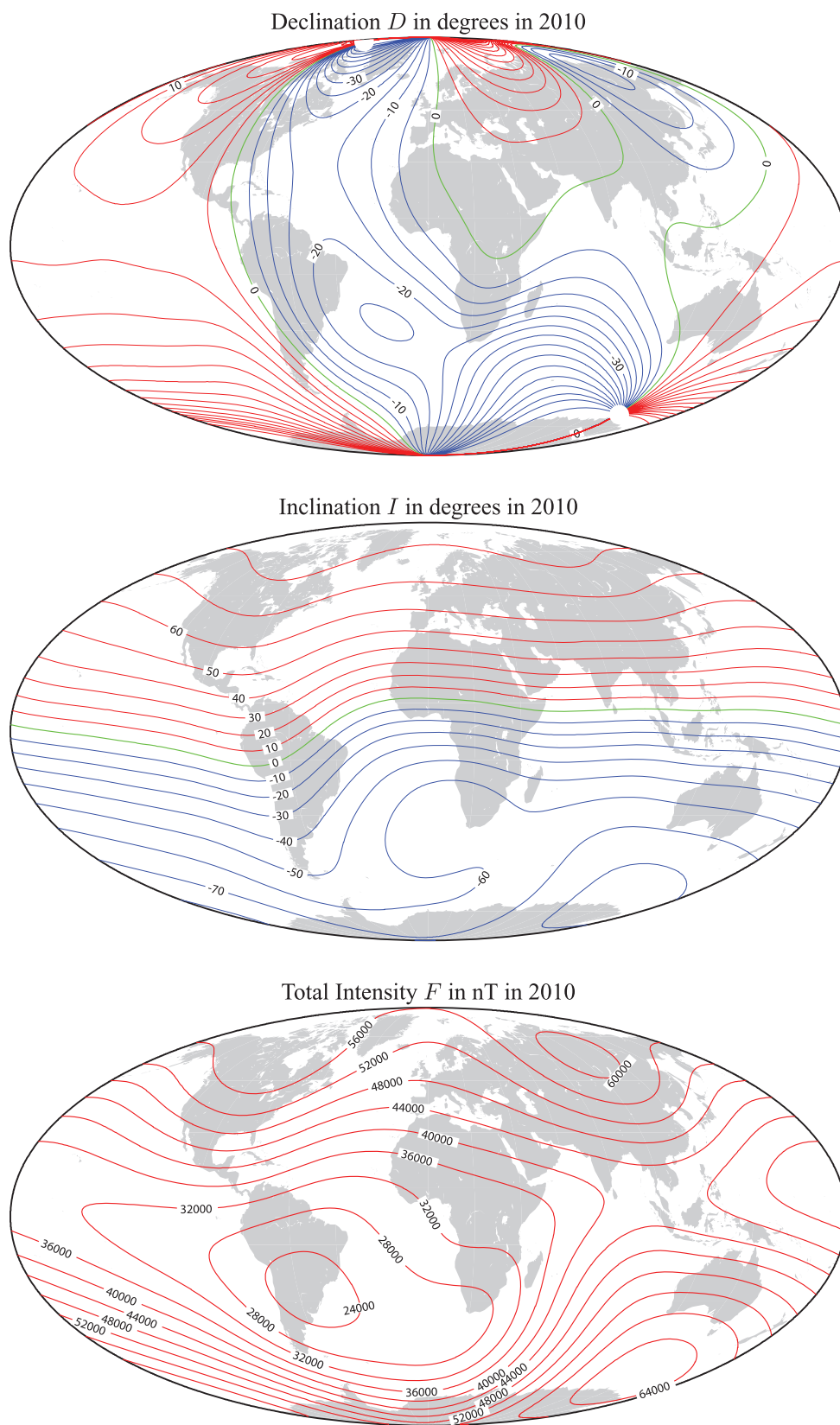
Figure 1. Maps of the magnetic declination *D* (top, units are degrees), inclination *I* (middle, units are degrees) and total intensity *F* (bottom, units are nT) at the Earth's surface in 2010 from the new field model IGRF 2010.0. Molleweide projection is used, zero line is shown in green, positive contours in red and negative contours in blue.

Predicted average change in Declination D in degrees/yr 2010-2015

Predicted average change in Inclination I in degrees/yr 2010-2015

Predicted average annual change in Total Intensity F in nT/yr 2010-2015
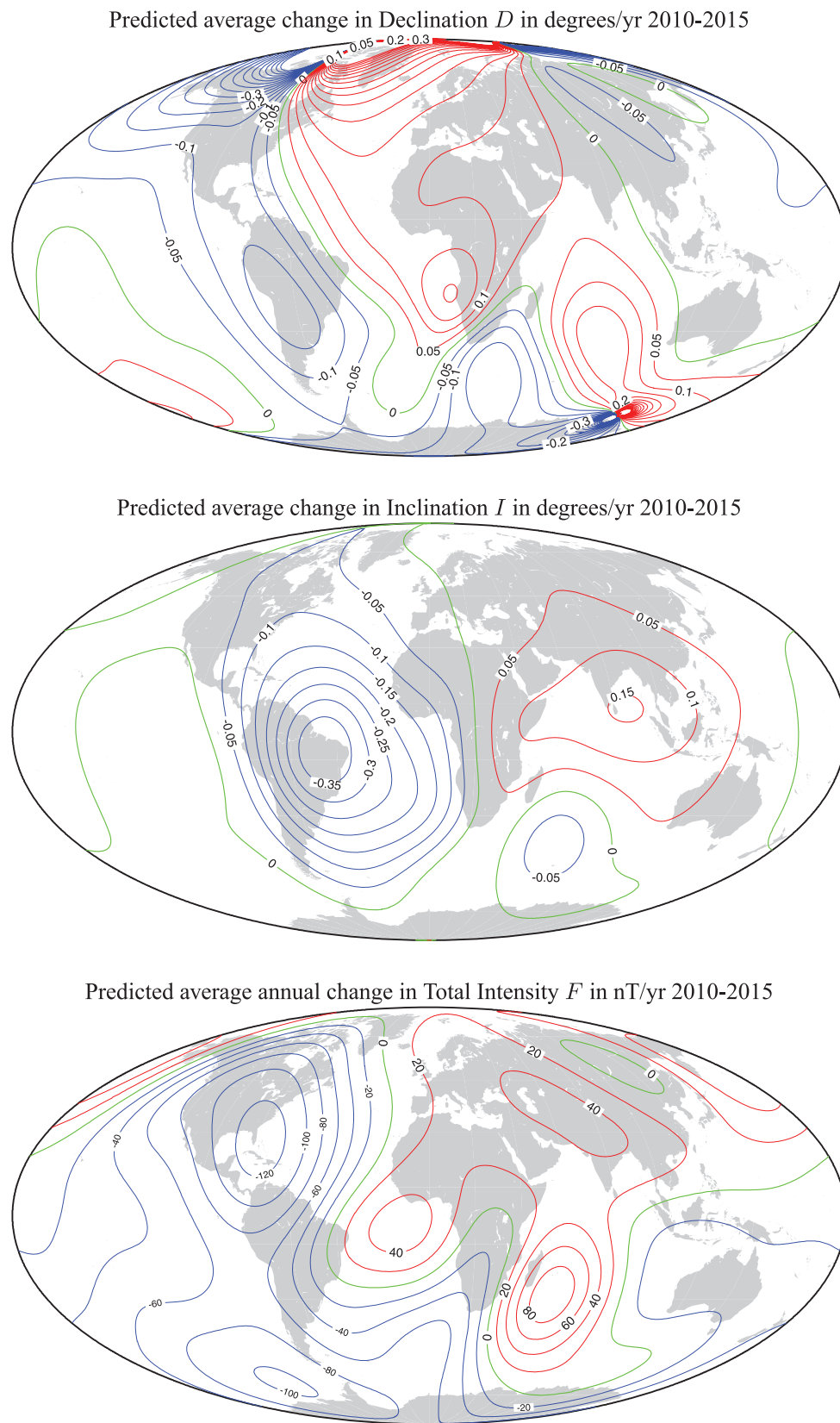
Figure 2. Maps of the predicted rate of change per year in the declination D (top, units are degrees yr^{-1}), the inclination I (middle, units are degrees yr^{-1}), and total intensity F (bottom, units are nT yr^{-1}) at the Earth's surface for the interval 2010–2015 as predicted by IGRF-11. Molleweide projection is used, zero line is shown in green, positive contours in red and negative contours in blue.
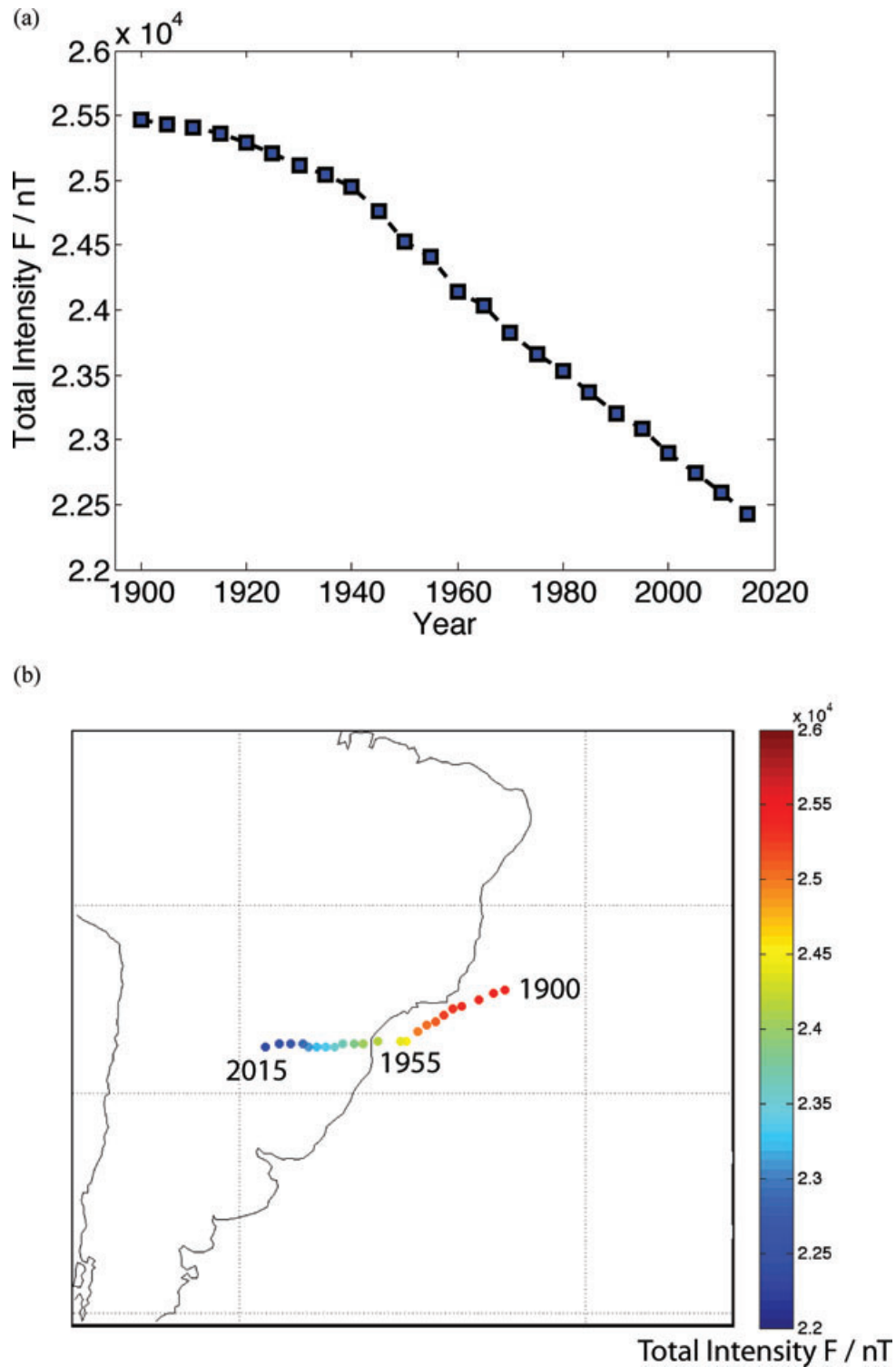
Figure 3. Evolution of the South Atlantic Anomaly during the 20th century: Top plot (a) shows how the minimum *F* at the Earth's surface (in the South Atlantic Anomaly where the magnitude of the field is smallest) has decreased from 1900 towards the present day, units are nT. The bottom plot (b) tracks the location of the point of lowest field magnitude with time; the colour scale indicates the magnitude of *F*, with blue representing smallest magnitude, units are nT.

Fortran software for synthesizing the field from the coefficients: http://www.ngdc.noaa.gov/IAGA/vmod/igrf11.f

C software for synthesizing the field from the coefficients (Linux): http://www.ngdc.noaa.gov/IAGA/vmod/geomag70_linux.tar.gz

C software for synthesizing the field from the coefficients (Windows): http://www.ngdc.noaa.gov/IAGA/vmod/geomag70_windows.zip

Online computation of field components from the IGRF-11 model: http://www.ngdc.noaa.gov/geomagmodels/IGRFWMM.jsp
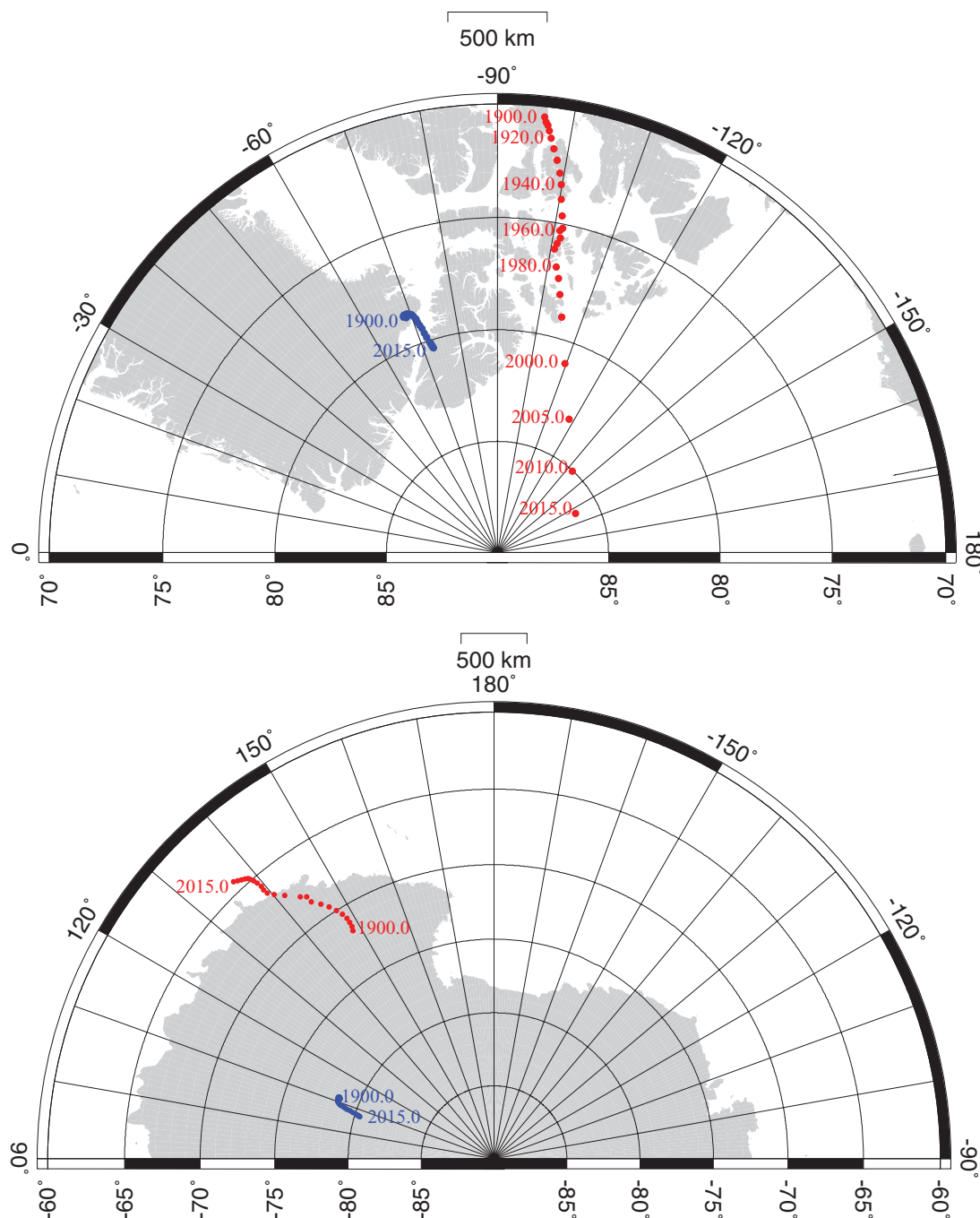
Figure 4. Motion of the magnetic dip pole (red) and geomagnetic pole (blue) since 1900 from IGRF-11 in the northern hemisphere (top) and the southern hemisphere (bottom). Stereographic projection is employed. The scale bar gives an indication of distance that is correct along lines of constant longitude and also along the middle lines of latitude shown.

http://www.geomag.bgs.ac.uk/gifs/igrf_form.shtml
http://wdc.kugi.kyoto-u.ac.jp/igrf/point/index.html

Archive of legacy versions of the IGRF model:
http://www.ngdc.noaa.gov/IAGA/vmod/igrf_old_models.html

Candidate models contributing to IGRF-11, and various test models are available for evaluation purposes:
http://www.ngdc.noaa.gov/IAGA/vmod/candidatemodels.html

Table 3. Magnetic pole positions since 1900 as determined from IGRF-11.

	North dip pole		South dip pole		North geomagnetic pole		South geomagnetic pole	
Epoch	Latitude	Longitude	Latitude	Longitude	Latitude	Longitude	Latitude	Longitude
1900.0	70.46	−96.19	−71.72	148.32	78.68	−68.79	−78.68	111.21
1905.0	70.66	−96.48	−71.46	148.55	78.68	−68.75	−78.68	111.25
1910.0	70.79	−96.72	−71.15	148.64	78.66	−68.72	−78.66	111.28
1915.0	71.03	−97.03	−70.80	148.54	78.64	−68.57	−78.64	111.43
1920.0	71.34	−97.39	−70.41	148.20	78.63	−68.38	−78.63	111.62
1925.0	71.79	−98.00	−69.99	147.63	78.62	−68.27	−78.62	111.73
1930.0	72.27	−98.69	−69.52	146.79	78.60	−68.26	−78.60	111.74
1935.0	72.80	−99.34	−69.06	145.77	78.57	−68.36	−78.57	111.64
1940.0	73.30	−99.87	−68.57	144.60	78.55	−68.51	−78.55	111.49
1945.0	73.93	−100.24	−68.15	144.44	78.55	−68.53	−78.55	111.47
1950.0	74.64	−100.86	−67.89	143.55	78.55	−68.85	−78.55	111.15
1955.0	75.18	−101.41	−67.19	141.50	78.54	−69.16	−78.54	110.84
1960.0	75.30	−101.03	−66.70	140.23	78.58	−69.47	−78.58	110.53
1965.0	75.63	−101.34	−66.33	139.53	78.60	−69.85	−78.60	110.15
1970.0	75.88	−100.98	−66.02	139.40	78.66	−70.18	−78.66	109.82
1975.0	76.15	−100.64	−65.74	139.52	78.76	−70.47	−78.76	109.53
1980.0	76.91	−101.68	−65.42	139.34	78.88	−70.76	−78.88	109.24
1985.0	77.40	−102.61	−65.13	139.18	79.04	−70.90	−79.04	109.10
1990.0	78.09	−103.68	−64.91	138.90	79.21	−71.13	−79.21	108.87
1995.0	79.09	−105.42	−64.79	138.76	79.39	−71.42	−79.39	108.58
2000.0	80.97	−109.64	−64.66	138.30	79.61	−71.57	−79.61	108.43
2005.0	83.19	−118.24	−64.55	137.85	79.82	−71.81	−79.82	108.19
2010.0	85.01	−132.66	−64.43	137.32	80.08	−72.22	−80.08	107.78
2015.0	86.07	−153.27	−64.30	136.74	80.36	−72.62	−80.36	107.38

REFERENCES

Barraclough, D.R., 1987. International Geomagnetic Reference Field: The Fourth Generation, *Phys. Earth. planet. Int.,* **48,** 279–292.

Barton, C.E., 1997. International Geomagnetic Reference Field: The Seventh Generation, *J. Geomag. Geoelect.,* **49,** 123–148.

Facius, R. & Reitz, G., 2007. Space weather impacts on space radiation protection, in *Space Weather, Physics and Effects,* pp. 289–352, eds Bothmer, V. & Daglis, I.A., Springer-Verlag, Berlin.

Finlay, C.C., Maus, S., Beggan, C., Hamoudi, M., Lowes, F.J., Olsen, N. & Thébault, E., 2010. Evaluation of candidate geomagnetic field models for IGRF-11, *Earth, Planets, Space,* submitted.

Friis-Christensen, E., Lühr, H. & Hulot, G., 2006. *Swarm:* a constellation to study the Earth's magnetic field, *Earth, Planets, Space.,* **58,** 351–358.

Gledhill, J.A., 1976. Aeronomic Effects of the South Atlantic Anomaly, *Rev. geophys. Space Phys.,* **14,** 173–187.

Heirtzler, J.R., 2002. The future of the South Atlantic Anomaly and implications for radiation damage in space, *J. Atmos. Solar-Terr. Phys.,* **64,** 1701–1708.

Hulot, G., Olsen, N. & Sabaka, T.J., 2007. The present field, geomagnetism, in *Treatise on Geophysics,* Vol. 5, pp. 33–75, ed. Schubert, G., Elsevier, Amsterdam.

IAGA Division I Study Group on Geomagnetic Reference Fields, 437-439. International Geomagnetic Reference Field 1975., *J. Geomag. Geoelect.,* **27,** 437–439.

Jackson, A., Jonkers, A.R.T. & Walker, M.R., 2000. Four centuries of geomagnetic secular variation from historical records, *Phil. Trans. R. Soc. Lond. A.,* **358,** 957–990.

Langel, R.A., 1992. International Geomagnetic Reference Field: The Sixth Generation, *J. Geomag. Geoelect.,* **44,** 679–707.

Langel, R.A., Barraclough, D.R., Kerridge, D.J., Golovkov, V.P., Sabaka, T.J. & Estes, R.H., 1988. Definitive IGRF models for 1945, 1950, 1955, and 1960., *J. Geomag. Geoelect.,* **40,** 645–702.

Lowes, F.J., 2000. An estimate of the errors of the IGRF/DGRF field 1945-2000, *Earth, Planets, Space,* **52,** 1207–1211.

Macmillan, S. & Finlay, C.C., 2010. The International Geomagnetic Reference Field, *IAGA Sopron Book Series,* in press.

Macmillan, S. *et al.,* 2003. The 9th-Generation International Geomagnetic Reference Field., *Geophys. J. Int.,* **155,** 1051–1056.

Macmillan, S., Turbitt, C. & Thomson, A., 2009. Ascension and Port Stanley geomagnetic observatories and monitoring the South Atlantic Anomaly, *Ann. Geophys.,* **52,** 83–95.

Mandea, M. & Macmillan, S., 2000. International Geomagnetic Reference Field – The Eighth Generation, 2000, *Earth. Planets, Space,* **52,** 1119–1124.

Maus, S. *et al.,* 2005a. The 10th-Generation International Geomagnetic Reference Field., *Geophys. J. Int.,* **161,** 561–565.

Maus, S., Macmillan, S., Lowes, F.J. & Bondar, T., 2005b. Evaluation of candidate geomagnetic field models for the 10th generation of IGRF, *Earth. Planet. Space,* **57,** 1173–1181.

Neubert, T. *et al.,* 2001. Ørsted satellite captures high-precision geomagnetic field data, *EOS, Trans. Am. geophys. Un.,* **82,** 81.

Newitt, L., Chulliat, A. & Orgeval, J.-J., 2009. Location of the north magnetic pole in april 2007, *Earth, Planets, Space,* **64,** 703–710.

Olson, P., 2007. Overview, core dynamics, in *Treatise on Geophysics,* Vol. 8, pp. 1–30, ed. Schubert, G., Elsevier, Amsterdam.

Peddie, N.W., 1982. International Geomagnetic Reference Field: The Third Generation, *J. Geomagn. Geoelect.,* **34,** 309–326.

Reigber, C., Lühr, H. & Schwintzer, P., 2002. CHAMP mission status, *Adv. Space Res.,* **30,** 129–134.

Winch, D.E., Ivers, D.J., Turner, J.P.R. & Stening, R.J., 2005. Geomagnetism and Schmidt quasi-normalization, *Geophys. J. Int.,* **160,** 487–504.

Zmuda, A.J., 1971. The International Geomagnetic Reference Field: Introduction, *Bull. Int. Assoc. Geomag. Aeronomy,* **28,** 148–152.

APPENDIX

World Data Centres

WORLD DATA CENTRE FOR GEOPHYSICS AND MARINE GEOLOGY, BOULDER
National Geophysical Data Center
E/GC 325 Broadway
Boulder, Colorado
USA 80305-3328
TEL: +01 303 497 6826
FAX: +01 303 497 6513
EMAIL: ngdc.info@noaa.gov
INTERNET: http://www.ngdc.noaa.gov/geomag/wdc/index.html

WORLD DATA CENTRE FOR GEOMAGNETISM, COPENHAGEN
DTU Space, Juliane Maries vej 30
DK-2100, Copenhagen
DENMARK
TEL: +45 3532 5700
FAX: +45 353 62475
EMAIL: jrgm@space.dtu.dk
INTERNET: http://www.space.dtu.dk/English/Research/Scientific_data_and_models

WORLD DATA CENTRE FOR GEOMAGNETISM, EDINBURGH
British Geological Survey
Murchison House, West Mains Road
Edinburgh, EH9 3LA
UNITED KINGDOM
TEL: +44 131 650 0234
FAX: +44 131 668 4368
EMAIL: wdcgeomag@bgs.ac.uk
INTERNET: http://www.wdc.bgs.ac.uk/catalog/master.html

WORLD DATA CENTRE FOR GEOMAGNETISM, KYOTO
Data Analysis Center for Geomagnetism and Space Magnetism
Graduate School of Science, Kyoto University
Kitashirakawa-Oiwake Cho, Sakyo-ku
Kyoto, 606-8502, JAPAN
TEL: +81 75 753 3929
FAX: +81 75 722 7884
EMAIL: iyemori@kugi.kyoto-u.ac.jp
INTERNET: http://wdc.kugi.kyoto-u.ac.jp

WORLD DATA CENTRE FOR GEOMAGNETISM, MUMBAI
Indian Institute of Geomagnetism
Colaba, Mumbai, 400 005, INDIA
TEL: +91 22 215 0293
FAX: +91 22 218 9568
EMAIL: abh@iigs.iigm.res.in
INTERNET: http://iigm.res.in

Table A1. List of agencies supporting observatories whose data were used in deriving constituent models for IGRF-11.

Supporting agencies	Country	Observatory IAGA code
Centre de Recherche en Astronomie, Astrophysique et Geophysique	ALGERIA	TAM
Universidad Nacional de la Plata	ARGENTINA	TRW
Geoscience Australia	AUSTRALIA	ASP, CNB, CSY, CTA, DVS, GNA, KDU, LRM, MAW, MCQ
Zentralanstalt für Meteorologie und Geodynamik	AUSTRIA	WIK
Institut Royal Météorologique	BELGIUM	DOU, MAB
CNPq-Observatório Nacional	BRAZIL	VSS
Academy of Sciences	BULGARIA	PAG
Geological Survey of Canada	CANADA	ALE, BLC, CBB, FCC, IQA, MEA, OTT, PBQ, RES, STJ, VIC,YKC
Academy of Sciences	CHINA	BMT
China Earthquake Adminstration	CHINA	CDP, CNH, GLM, GZH, KSH, LZH, MZL, QGZ, QIX, SSH, THJ, WHN
Instituto Geográfico Agustín Codazzi	COLOMBIA	FUQ
Academy of Sciences	CZECH REPUBLIC	BDV
Danish Meteorological Institute / DTU Space	DENMARK	BFE, GDH, NAQ, THL
Addis Ababa University	ETHIOPIA	AAE
Finnish Meteorological Institute	FINLAND	NUR
Geophysical Observatory	FINLAND	SOD
Institut de Physique du Globe de Paris	FRANCE	AAE, BOX, CLF, KOU, LZH,PHU, QSB, PPT, TAM
Ecole et Observatoire des Sciences de la Terre	FRANCE	AMS, CZT, DRV, PAF, TAN
Institut Français de Recherche Scientifique pour le Développement	FRANCE	BNG, MBO

Table A1. (*Continued.*)

Supporting agencies	Country	Observatory IAGA code
Academy of Sciences	GEORGIA	TFS
Universität München	GERMANY	FUR
Alfred-Wegener-Institute for Polar Marine Research &	GERMANY	VNA
GFZ Hemholtz Centre Potsdam	GERMANY	NGK, WNG
Universität Stuttgart	GERMANY	BFO
Institute of Geology and Mineral Exploration	GREECE	PEG
Academy of Sciences	HUNGARY	NCK
Eötvös Loránd Geophysical Institute	HUNGARY	THY
University of Iceland	ICELAND	LRV
Indian Institute of Geomagnetism	INDIA	ABG, NGP, PND, SIL, TIR, UJJ, VSK
Badan Meteorologi dan Geofisika	INDONESIA	TND, TUN
Meteorological Service	IRELAND	VAL
Survey of Israel	ISRAEL	AMT, BGY, ELT
Instituto Nazionale di Geofisica e Vulcanologia	ITALY	AQU
Japan Coast Guard	JAPAN	HTY
Japan Meteorological Agency	JAPAN	CBI, KAK, KNY, MMB
Geographical Survey Institute	JAPAN	ESA, KNZ, MIZ
Science for Institute of the Ionosphere	KAZAKHSTAN	AAA
National Centre for Geophysical Research	LEBANON	QSB
Université dAntananarivo	MADAGASCAR	TAN
Universidad Nacional Autonoma de México	MEXICO	TEO
Institute of Geological and Nuclear Sciences	NEW ZEALAND	API, EYR, SBA
University of Tromsø	NORWAY	BJN, DOB, TRO
Instituto Geofisico del Peru	PERU	HUA
Academy of Sciences	POLAND	BEL, HLP, HRN
Directorate General of Telecommunications	REPUBLIC OF CHINA	LNP
Instituto Nacional de Geologia	REPÚ BLICA DE MOÇAMBIQUE	LMM
Geological Survey of Romania	ROMANIA	SUA
Academy of Sciences	RUSSIA	ARS, BOX, LVV, MOS, NVS
Institute of Solar-Terrestrial Physics	RUSSIA	IRT
Dept. of Agriculture, Forestry, Fisheries & Meteorology	SAMOA	API
Geomagnetic College Grocka	SERBIA & MONTENEGRO	GCK
Slovenska Akademia Vied	SLOVAKIA	HRB
National Research Foundation	SOUTH AFRICA	HBK, HER, TSU
Observatori de lEbre	SPAIN	EBR, LIV
Real Instituto y Observatorio de la Armada	SPAIN	SFS
Instituto Geográfico Nacional	SPAIN	GUI, SPT
Sveriges Geologiska Undersökning	SWEDEN	ABK, LOV, UPS
Swedish Institute of Space Physics	SWEDEN	KIR
Bŏgaziçi University	TURKEY	IZN
Academy of Sciences	UKRAINE	AIA
British Geological Survey	UNITED KINGDOM	ASC, ESK, HAD, LER, PST
US Geological Survey	UNITED STATES	BRW, BOU, BSL, CMO, DLR, FRD, FRN, GUA HON, MID, NEW, SIT, SJG, SHU, TUC
Academy of Science and Technology	VIETNAM	PHU